GEOPHYSICS, VOL. 62, NO. 5 (SEPTEMBER-OCTOBER 1997); P. 1596–1611, 18 FIGS.

Estimation of multiple scattering by iterative inversion, Part II: Practical aspects and examples

D. J. Verschuur* and A. J. Berkhout*

ABSTRACT

A surface-related multiple-elimination method can be formulated as an iterative procedure: the output of one iteration step is used as input for the next iteration step (part I of this paper). In this paper (part II) it is shown that the procedure can be made very efficient if a good initial estimate of the multiple-free data set can be provided in the first iteration, and in many situations, the Radon-based multiple-elimination method may provide such an estimate. It is also shown that for each iteration, the inverse source wavelet can be accurately estimated by a linear (least-squares) inversion process. Optionally, source and detector variations and directivity effects can be included, although the examples are given without these options. The iterative multiple elimination process, together with the source wavelet estimation, are illustrated with numerical experiments as well as with field data examples. The results show that the surface-related multiple-elimination process is very effective in time gates where the moveout properties of primaries and multiples are very similar (generally deep data), as well as for situations with a complex multiple-generating system.

INTRODUCTION

Preliminary work on the surface-related multiple problem can already be found in Anstey and Newman (1967), who observed that by autoconvolving seismic traces multiples could be better visualized. Riley and Clearbout (1976) described a forward model of surface-related multiples for a 2-D medium, but could not come yet to a proper inverse scheme to remove them from the data. The theory of surface-related multiple removal has been described in Kennett (1979) for 1-D media and Berkhout (1982) for multidimensional media. In Berkhout's formulation, data acquisition parameters are included and the multiples related to the free surface are estimated using the data itself as the multidimensional prediction operator. Therefore, information from the subsurface is not required in this method, but the inverse source wavefield should be accurately known. An adaptive version of the surface-related multiple removal procedure with successful applications to field data has been developed in recent years (Verschuur et al., 1992). The predicted multiples are adaptively subtracted from the input data, as an accurate source wavefield description is generally not available.

In part I of this paper (Berkhout and Verschuur, 1997, also in this issue), the surface-related multiple-elimination process has been described as an iterative inversion procedure. In this paper, we will take a look at the practical aspects of this formulation based on numerically simulated and field data examples. The influence of choosing different initial multiple-free estimates is investigated and several practical issues are discussed. Both the simulated and the field data examples show that a good initial estimate of the multiple-free data is not necessary but it speeds up the iteration process.

ITERATIVE MULTIPLE-ELIMINATION PROCEDURE

The principal iterative equation, as described in part I of this paper, can be given as (we omit the depth level indication for notational simplicity)

$$\underset{\sim}{\mathbf{P}}_0^{(n+1)} = \underset{\sim}{\mathbf{P}} - \underset{\sim}{\mathbf{P}}_0^{(n)} \underset{\sim}{\mathbf{A}}^{(n+1)} \underset{\sim}{\mathbf{P}}. \tag{1}$$

Matrix $\underset{\sim}{\mathbf{P}}$ represents one Fourier component of the input data with all multiples, $\underset{\sim}{\mathbf{P}}_0^{(n)}$ contains the nth estimate of the multiple-free data, $\underset{\sim}{\mathbf{A}}$ is the surface operator, and $\underset{\sim}{\mathbf{P}}_0^{(n+1)}$ gives the (updated) multiple-free data for this iteration (i.e. the $n+1$th iteration). The matrix notation as defined in Berkhout (1982) can in principle handle both 3-D and 2-D seismic data. However, in this paper we will restrict ourselves to the 2-D situation. This means that each column of the data matrix $\underset{\sim}{\mathbf{P}}$ contains a 2-D shot record for one frequency (or Laplace) component. The data matrix $\underset{\sim}{\mathbf{P}}$ can be expressed in terms of the subsurface

Manuscript received by the Editor July 24, 1995; revised manuscript received June 27, 1996.
*Delft University of Technology, Centre of Technical Geoscience, Laboratory of Seismics and Acoustics, P.O. Box 5046, 2600 GA Delft, The Netherlands. E-mail addresses: d.j.verschuur@ctg.tudelft.nl; berkhout@dutnak2.tn.tudelft.nl.

impulse response $\underset{\sim}{\mathbf{X}}$ and the source and receiver properties (see also part I of this paper) as

$$\underset{\sim}{\mathbf{P}} = \underset{\sim}{\mathbf{D}}^{-}\underset{\sim}{\mathbf{X}}\underset{\sim}{\mathbf{S}}^{+}, \tag{2}$$

where $\underset{\sim}{\mathbf{S}}^{+}$ is the downgoing source wavefield matrix (including all array and surface interaction effects) and $\underset{\sim}{\mathbf{D}}^{-}$ representing the operator that converts the upgoing pressure wavefield to actual measurements (e.g., total pressure for marine data or vertical velocity component for land data). Note that each column of the data matrices contains one Fourier (or Laplace) component of a shot record. The surface operator $\underset{\sim}{\mathbf{A}}$ is expressed as the combination of the free-surface reflectivity, the inverse source wavefield and the inverse detector operator:

$$\underset{\sim}{\mathbf{A}} = \left[\underset{\sim}{\mathbf{S}}^{+}\right]^{-1}\underset{\sim}{\mathbf{R}}^{-}\left[\underset{\sim}{\mathbf{D}}^{-}\right]^{-1}, \tag{3}$$

such that it couples the two wavefields in expression (1), $\underset{\sim}{\mathbf{P}}_0^{(n)}$ and $\underset{\sim}{\mathbf{P}}$, with the surface reflectivity, removing the influence of sources and receivers. This surface operator can be chosen different for each iteration. If we start with an initial estimate of the multiple-free data $\hat{\underset{\sim}{\mathbf{P}}}_0$, then the first iteration results in

$$\underset{\sim}{\mathbf{P}}_0^{(1)} = \underset{\sim}{\mathbf{P}} - \left[\hat{\underset{\sim}{\mathbf{P}}}_0\underset{\sim}{\mathbf{A}}^{(1)}\right]\underset{\sim}{\mathbf{P}}, \tag{4}$$

and the second iteration results in

$$\underset{\sim}{\mathbf{P}}_0^{(2)} = \underset{\sim}{\mathbf{P}} - \left[\underset{\sim}{\mathbf{P}}\underset{\sim}{\mathbf{A}}^{(2)}\right]\underset{\sim}{\mathbf{P}} + \left[\hat{\underset{\sim}{\mathbf{P}}}_0\underset{\sim}{\mathbf{A}}^{(1)}\right]\left[\underset{\sim}{\mathbf{P}}\underset{\sim}{\mathbf{A}}^{(2)}\right]\underset{\sim}{\mathbf{P}}, \tag{5}$$

etc. From equation (5) it is clear that, assuming the initial estimate of the multiple-free data is not perfect, after each iteration the influence of the initial estimate shifts toward the higher order multiples. Therefore, we can allow working with a "bad" initial multiple-free estimate. For instance, if one starts with $\hat{\underset{\sim}{\mathbf{P}}}_0 = \underset{\sim}{\mathbf{0}}$, then $\hat{\underset{\sim}{\mathbf{P}}}_0^{(1)} = \underset{\sim}{\mathbf{P}}$ and $\hat{\underset{\sim}{\mathbf{P}}}_0^{(n)}$ is given by n terms of the Neumann series expansion of the exact solution (see part I of this paper). However, we will show that a good initial estimate will improve the convergence of the iteration process.

FULL ADAPTIVE PROCEDURE

As the surface operator $\underset{\sim}{\mathbf{A}}$ is not known in advance, it can be estimated by assuming that after multiple removal the total amount of energy in the seismic data is minimum. Although it is possible to construct hypothetical situations where this is not the case, it is a well-accepted criterion used in many adaptive multiple removal schemes, like prediction error filtering [Robinson and Treitel (1980)] and wave-equation–based multiple removal [for example, Berryhill and Kim (1986), and Wiggins (1988)].

In the general case, the surface operator $\underset{\sim}{\mathbf{A}}$ is not a simple diagonal matrix, but can be considered to be a band matrix, describing the inverse source and receiver directivity correction filters. According to Fokkema et al. (1990) the size of the band is in the order of 20. Using exact expression (1), we have to solve at each frequency for the unknown (band) matrix $\underset{\sim}{\mathbf{A}}(\omega)$ such that the total energy in the output is minimized:

$$E = \sum_{\omega,i,j} |\{\underset{\sim}{\mathbf{P}}(\omega)\}_{i,j} - \{\hat{\underset{\sim}{\mathbf{P}}}_0(\omega)\underset{\sim}{\mathbf{A}}(\omega)\underset{\sim}{\mathbf{P}}(\omega)\}_{i,j}|^2 \quad is\ minimum, \tag{6}$$

including the constraint that the operator $\underset{\sim}{\mathbf{A}}$ is short in the time domain (smoothness constraint in the frequency domain). This estimation process is, however, very elaborate and is currently under investigation. By taking some assumptions on the source and receiver operators, the optimization procedure simplifies dramatically.

SIMPLIFIED ADAPTIVE PROCEDURE

If we may assume $\underset{\sim}{\mathbf{R}}^{-} = -\mathbf{I}$, then an estimation of $\underset{\sim}{\mathbf{A}}$ means an estimation of $[\underset{\sim}{\mathbf{D}}^{-}\underset{\sim}{\mathbf{S}}^{+}]^{-1}$. In addition, if we may assume dipole sources and assume that the receiver directivity (including the so-called ghost effect) have been corrected for in advance (or just neglect them), then $\underset{\sim}{\mathbf{A}}$ can be represented by a diagonal matrix, containing the source and /or receiver transfer functions (for one frequency) at the diagonal. Finally, if we may also assume that sources and detectors do not show any variations during the seismic survey, then $\underset{\sim}{\mathbf{A}}$ may be represented by a scaled unity matrix, the scaling factor defining one Fourier (or Laplace) component of the inverse of the effective source and receiver signature as

$$\underset{\sim}{\mathbf{A}} = \underset{\sim}{\mathbf{A}}(\omega) \approx A(\omega)\underset{\sim}{\mathbf{I}} = -[D^{-}(\omega)S^{+}(\omega)]^{-1}\underset{\sim}{\mathbf{I}}. \tag{7}$$

Expression (7) plays an important role in this paper.

If simplifying assumption (7) is used, the iterative procedure simplifies to

$$\underset{\sim}{\mathbf{P}}_0^{(n+1)} = \underset{\sim}{\mathbf{P}} - A^{(n+1)}(\omega)\underset{\sim}{\mathbf{P}}_0^{(n)}\underset{\sim}{\mathbf{P}}. \tag{8}$$

We will demonstrate that simplifying assumption (8) still yields very good results on simulated and field data. The resulting multiple-elimination scheme consists of three basic steps in each iteration:

1) Prediction of the "unscaled" multiples, using the current estimate of the multiple-free data and the input data, according to

$$\underset{\sim}{\mathbf{M}}^{(n+1)} = \underset{\sim}{\mathbf{P}}_0^{(n)}\underset{\sim}{\mathbf{P}}. \tag{9}$$

2) Inverse transformation of this multiple data to the time domain by combining all frequencies to obtain

$$m^{(n+1)}(t, x_r, x_s) = FT^{-1}\{\underset{\sim}{\mathbf{M}}^{(n+1)}\}, \tag{10}$$

where x_r and x_s are the (discrete) receiver and source positions of the seismic traces.

3) Least-squares estimation of a short operator $a^{(n+1)}(t)$ to minimize the energy in the result after subtraction of the estimated multiples $m^{(n+1)}(t, x_r, x_s)$ from the input data $p(t, x_r, x_s)$ to obtain

$$E = \sum_{t,x_r,x_s} \left[p(t, x_r, x_s) - a^{(n+1)}(t) * m^{(n+1)}(t, x_r, x_s)\right]^2. \tag{11}$$

For the filtering procedure a standard Wiener-shaping filter can be used (Robinson and Treitel, 1980). Note that the filter $a^{(n+1)}(t)$ is a wavelet deconvolution filter, i.e., it will transform the wavelet in the primary estimate $\mathbf{P}_0^{(n)}$ into a band-limited spike, such that the resulting wavefield approaches a true impulse response.

ADAPTIVE FILTERING STRATEGY

In general, there will be limitations on the proposed adaptive procedure:

1) Although the theoretical description holds for both 2-D and 3-D data, in practice it is applied to data recorded along a line. Therefore, because of 3-D medium variations, the predicted multiples will not match the true multiples completely.
2) The geometrical spreading on field data is 3-D and not 2-D.
3) The method assumes a receiver position at each source position and vice versa. Because a near offset gap is always present, missing traces need to be reconstructed. For the field data examples in this paper, the method described in Kabir and Verschuur (1995) has been used. However, such a reconstruction method always has some limitations that will result in an imperfect multiple prediction.

Therefore, in practice the method requires a more adaptive filtering procedure to overcome some of the limitations mentioned. This can be achieved by

1) Minimizing equation (11) per shot record:

$$E\left(x_s^{(i)}\right) = \sum_{t,x_r} \left[p\left(t, x_r, x_s^{(i)}\right) - a_i^{(n+1)}(t) * m_0^{(n+1)}\left(t, x_r, x_s^{(i)}\right)\right]^2 \; is\; minimum, \quad (12a)$$

or per detector gather:

$$E\left(x_r^{(j)}\right) = \sum_{t,x_s} \left[p\left(t, x_r^{(j)}, x_s\right) - a_j^{(n+1)}(t) * m_0^{(n+1)}\left(t, x_r^{(j)}, x_s\right)\right]^2 \; is\; minimum, \quad (12b)$$

or doing both.
2) Minimizing equation (11) within time and/or offset windows in each shot gather, receiver gather, or even common offset gather.

Although a strict physical meaning to these adaptive filtering procedures cannot be assigned anymore, they are meant to overcome small deviations in the seismic data model from the assumptions that have been made. In general, the strategy to follow is to estimate a long filter (i.e., typical 21 to 31 points) for optimization per shot gather and use that result for a second adaptation step within local time and/or offset windows with smaller filters (i.e., typical 5 points). After processing a data set in this way, the estimated filter per shot gather can be used as a quality control measure, and in situations where some of the assumptions were not well met, variations in the estimated filters can be observed (although the contrary does not need to be true). Of course, the more local the adaptation is applied, the higher the chance that the minimum-energy assumption is violated. Therefore, a critical testing for each data set is needed.

In the following sections, our strategy is illustrated with some examples.

NUMERICAL EXPERIMENTS

Example with a horizontally layered model

As a first illustration of the iterative multiple elimination process, we consider the very simple subsurface model of Figure 1. Note that this is the same subsurface model as has been used in Part I of this paper. Using a zero-phase wavelet (see Figure 2d and 2e), the modeled data with multiples, "primaries only" and "multiples only" are displayed in Figure 2a through 2c. For simulating this data, the so-called "reflectivity" method in the wavenumber-frequency domain is used, which calculates 2-D (i.e., line source) amplitudes. Note that the energy of the multiples is quite large compared to the primaries. We can also discover surface-related multiples, that are not related to the first reflector (e.g., at 0.9 s we can distinguish the surface-multiple of the second reflector with itself, and at 1.15 s a surface multiple that has bounced against the second and the third reflector). These multiples are generally very difficult to remove with standard multiple-elimination methods.

To this data the iterative procedure will be applied with different choices of the initial multiple-free estimate, according to equation (1). For the iterative procedure, we assume that the seismic line consists of identical shot records, such that the matrix multiplications in equation (9) can be replaced by scalar multiplications in the wavenumber-frequency domain. For each iteration, one global surface operator $a(t)$ is estimated, by minimizing the energy in the complete shot gather. After a few iterations, we expect that this operator will converge to the correct inverse source signature (within the frequency band of the data).

Input data as initial primary estimate.—The first estimate for the initial multiple-free data is chosen to be the data itself ($\mathbf{P}$). Of course, this is not the most intelligent choice and, therefore, will yield nonoptimal convergence speed. Figure 3 shows the first three iterations of the iterative multiple elimination procedure. After three iterations, the result is satisfactory. At each iteration, a different surface operator $a(t)$ is allowed (with 15 points length). The resulting operators for each iteration are displayed in Figure 3d and 3e for the amplitude and phase spectrum, respectively. For the frequency-domain plots, null samples have been padded to the original trace length to achieve a smooth amplitude and phase function display. Although the amplitude spectrum changes with each iteration step resulting from the imperfect nature of the estimate of the multiple-free data, it converges to the correct inverse wavelet spectrum. Note that the phase spectrum is already correct from the first iteration on, although we did not put any restriction on the phase. It emphasizes the sensitivity of the multiple-elimination procedure for estimating the phase spectrum of the source signature.

Muted Radon output as initial primary estimate.—From the literature, it is well known that the parabolic Radon transform is generally very effective in separating primaries and multiples

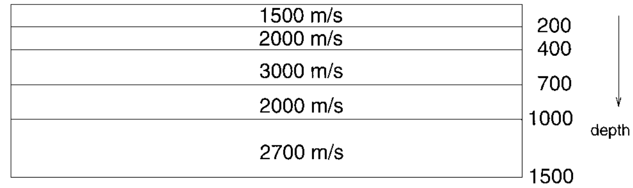

FIG. 1. One-dimensional subsurface model with three horizontal reflectors.

at shallow levels, where there is enough velocity discrimination (Hampson, 1986). Hence, the muted output of the Radon-based multiple suppression process may define, with respect to the previous choice, a better initial estimate for our iterative surface-related algorithm. Figure 4a shows the Radon output and, as expected, the shallow part is already a good estimate of the multiple-free data. Figure 4b shows that one iteration already produces a very satisfactory result, and the output of the second iteration is nearly perfect. As expected, the estimated inverse source signature (Figure 4d and 4e) is already correct at the first iteration.

Example with a complex sea bottom

For the next example we consider the subsurface model as shown in Figure 5. It contains significant lateral variations in the water bottom topography. Most multiple removal schemes will not work on this data because of its complex multiple-generating system. Using a wavelet, which has been extracted from an air-gun–array field measurement (see Figure 6), shot records have been modeled with a 2-D recursive extrapolation procedure in the $x - \omega$ domain. The line consists of 141 shot records with 101 receivers in an in-line marine spread configuration, with the spacing between shots and receivers being 15 m. The seismic modeling has been done for the situations with all multiples and without the surface-related multiples for the reference output. One shot record, with the source at $x = 1050$ m (as indicated with the circle in Figure 5), and the zero offset section have been displayed in Figure 7, both for situations with and without surface-related multiples. Note that the multiples show a very complex behavior, in the shot gather as well as in the zero-offset section. Note, in particular, the

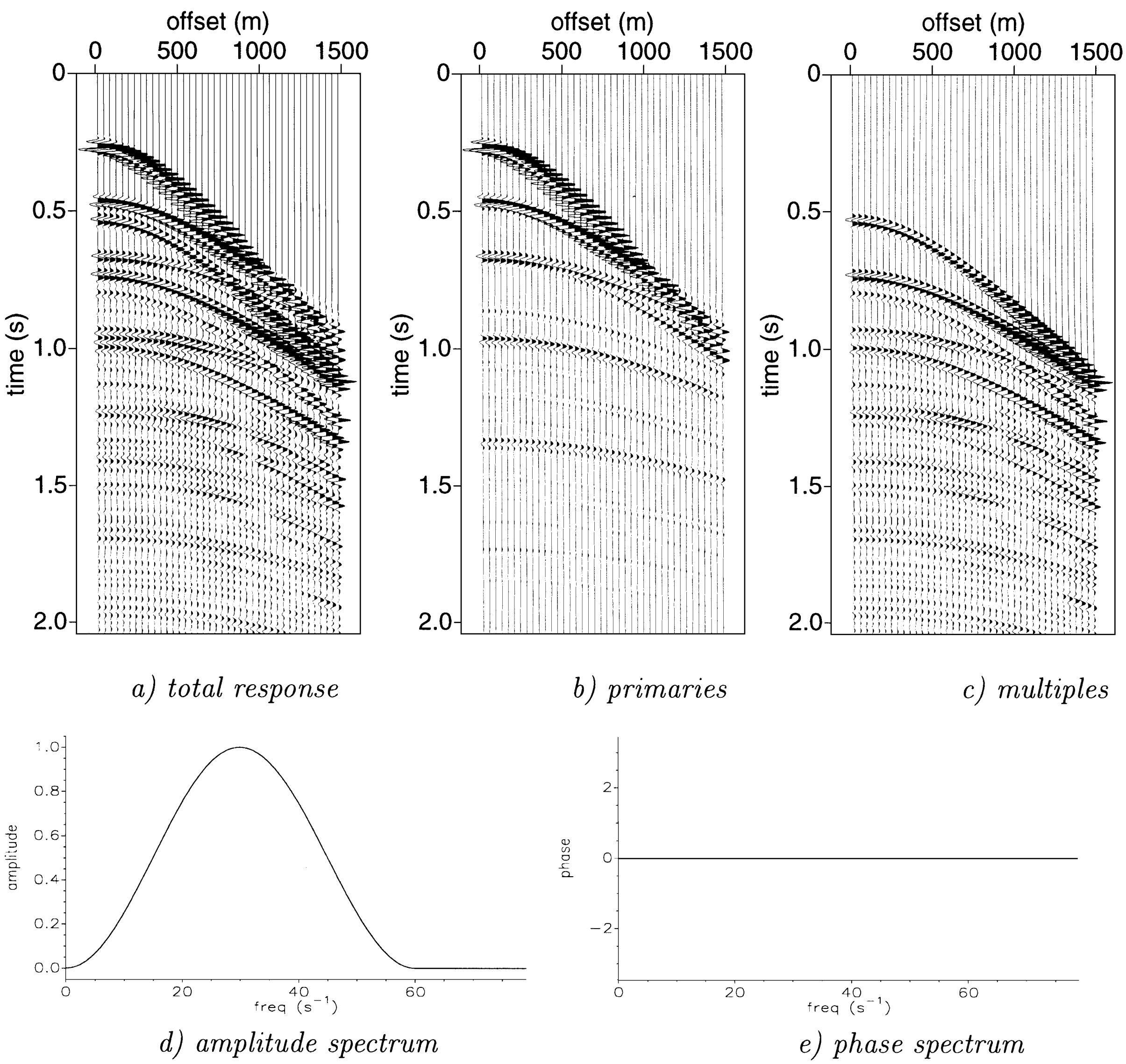

FIG. 2. Shot records related to the three-reflector model of Figure 1. (a) Shot record with multiples. (b) Shot record modeled without surface-related multiples. (c) Surface-related multiples, i.e., difference of (a) and (b). Amplitude (d) and phase (e) spectrum of the zero phase, cosine-square–shaped wavelet that is used to band limit the data.

focusing and diffraction effects caused by the fast variations in the water-bottom topography at lateral position 1600 m.

Input data as initial primary estimate.—Applying the adaptive surface-related multiple procedure with the input data as initial multiple-free estimate, the first iteration already shows a surprisingly good result, which can be seen in the upper part of Figure 8. The second iteration is visible in the lower part of Figure 8. Some remaining multiple energy visible in Figure 8a and 8b (e.g., below position 1600 m) is removed after the second iteration. This appears to be from second and higher order multiples. Furthermore, it is clear that primary information is preserved after the multiple-elimination process. Note the artificial diffraction events in the output visible at the edges of the data sets for both iterations. They are caused by the limited aperture of this small scale experiment (end-effects). As the method involves spatial convolutions of the shot records with themselves, the last shot record at each side of the line will act as a source of diffractions (truncation effects). They are only visible in the outer shot records of a line, however, for field data our experience is that they are generally weak. Because of truncation effects, the effectiveness of the removal with the minimum energy criterion has been decreased in our synthetic example. This results in the small multiple remaining, e.g., below the synclinal structures at $x = 800$ and $x = 1600$ m. The energy of these nonremoved multiples is thus similar to the energy of the created artifacts.

The adaptive multiple subtraction for each iteration has been done in two steps:

1) First, a global inverse source signature $a(t)$ has been found by minimizing the energy given by equation (12a) for all shot records simultaneously. This yields one version of $a(t)$ for each iteration.

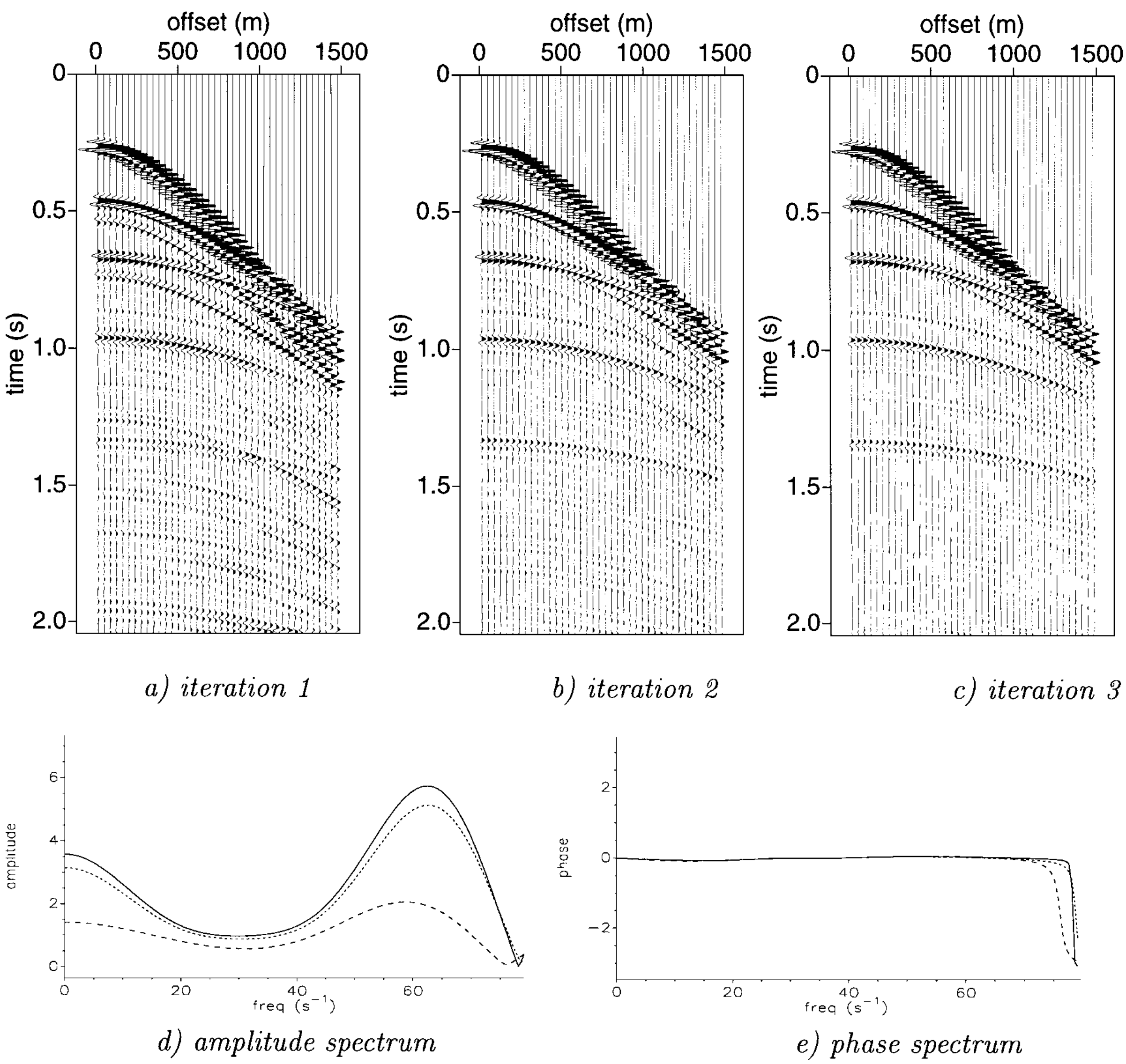

FIG. 3. Result for three iterations of the multiple removal process using the input data (Figure 2a) as initial multiple-free estimate. Amplitude (d) and phase (e) spectrum of the estimated inverse source signatures per iteration (solid line is the third iteration).

2) Second, after deconvolution with this filter, the multiples are subtracted adaptively in time windows in the order of 400 ms to get an improved "local" adaptation. For each time window, a 3-point filter is estimated, which merely allows an additional amplitude scaling and a slight phase shift.

To check the validity of the estimated $a(t)$ in the first adaptation step (global step), $a(t)$ is convolved with the original source signature. Figure 9 shows the deconvolution result for both iterations. As expected, even a very wrong estimate of the initial multiple-free estimate results in a very good inverse source signature estimate—the deconvolution result is close to a zero-phase signal with a unit amplitude spectrum within the bandwidth of the data. Note that the first iteration result (dashed line) has a small overall amplitude error. However, the phase spectrum is already correct at the first iteration!

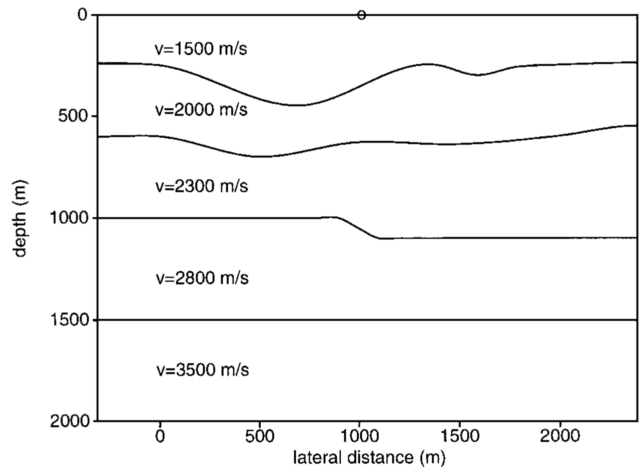

FIG. 5. Subsurface model with laterally varying sea bottom.

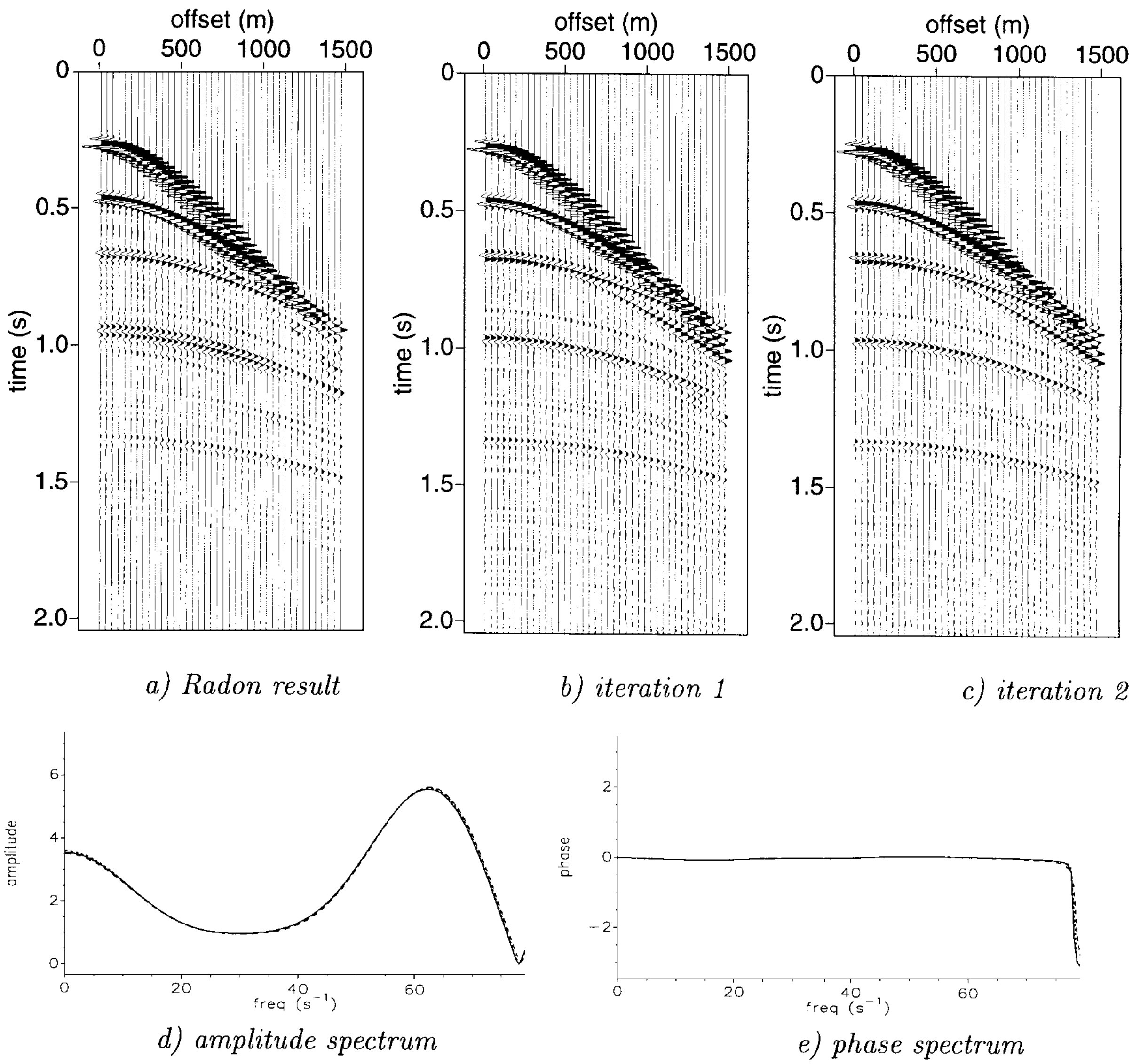

FIG. 4. (a) Initial estimate of the multiple-free data: output of parabolic Radon filtering. (b) First iteration result using this as initial multiple free data. (c) Second iteration result. Amplitude (d) and phase (e) spectrum of the estimated inverse source signatures per iteration (solid line is the third iteration).

Muted Radon output as initial primary estimate.—The best initial multiple-free estimate is expected when we use the shallow output of the parabolic Radon multiple-elimination method. However, for this complex sea-bottom geometry, the common-midpoint–(CMP) oriented Radon method does not work properly, as the parabolic assumption of (multiple) events in the Radon domain is not valid here. Still we use the parabolic Radon method as a start, but mute all events from the second reflector onward (below the second reflector we noticed serious problems with the Radon multiple-elimination method). Using the Radon-based estimate, the iterative multiple-elimination procedure is applied. Figure 10 shows the first two iterations for the selected shot record and the zero-offset section. Compared to the previous results, where the data itself was used as initial multiple-free estimate, a (slight) improvement can be observed for the first iteration (second-order multiples below position 1600 m). Note also that the edge effects have been reduced. The output of the second iteration is similar for both initial estimates. Although using the Radon initial estimate shows an acceptable result after one iteration, for the shots near the edges a second iteration is advisable.

Figure 11 shows the result of convolving $a(t)$ with the original source signature. Both iterations show a good result. Looking at the deconvolution result, the shallow Radon output serves as a better initial multiple-free estimate than the seismic data itself.

From the two simulated data examples, we may conclude that the shallow output of Radon multiple elimination yields a good initial estimate. However, for very complex structures the advantage of Radon preprocessing disappears.

FIELD DATA EXAMPLE

North Sea data set

The field data set under consideration is taken from a survey in the North Sea with a water depth of approximately 300 m. Here we show the validity of the iterative procedure to field data, again using the full input data and the output of parabolic Radon filtering as initial estimate for the multiple-free data. The results will be compared for a shot gather and for the CMP stack.

Input data as initial primary estimate.—Figure 12a shows a shot gather after some basic preprocessing (direct wave mute, missing near-offset interpolation). The shot position corresponds with CMP 1250 in the stacked sections. For all shot record displays, a normal moveout (NMO) correction has been applied to emphasize the primary events, which should appear more or less as horizontal events (the dips in this section are small). First, the input data is used directly as initial estimate. With the iterative multiple-elimination procedure, the predicted multiples for the first iteration are calculated. During this process, deghosting at the receivers has been included to make sure that the predicted multiples obtain the same receiver characteristics as the true multiples.

The next step of the elimination procedure is to subtract the predicted multiples in an adaptive way from the input data, estimating the inverse source signature $a(t)$. Similar to the complex water-bottom example, the subtraction is done in two stages: first, a global inverse source signature should be found for all shot records simultaneously and then allow a smooth time-varying adaptation. Figure 12b shows this result for the one-shot gather under consideration, with the difference plot in Figure 12c, being the multiples removed in iteration 1. Next, in the second iteration, this output is used as a multiple-prediction operator, and the result is shown in Figure 12d. Figure 12e shows the difference between Figure 12a and 12d. Note that after one iteration, a good result is already obtained. It is interesting to see that with the second iteration, the subtracted multiples (Figure 12e) show an emphasis on the

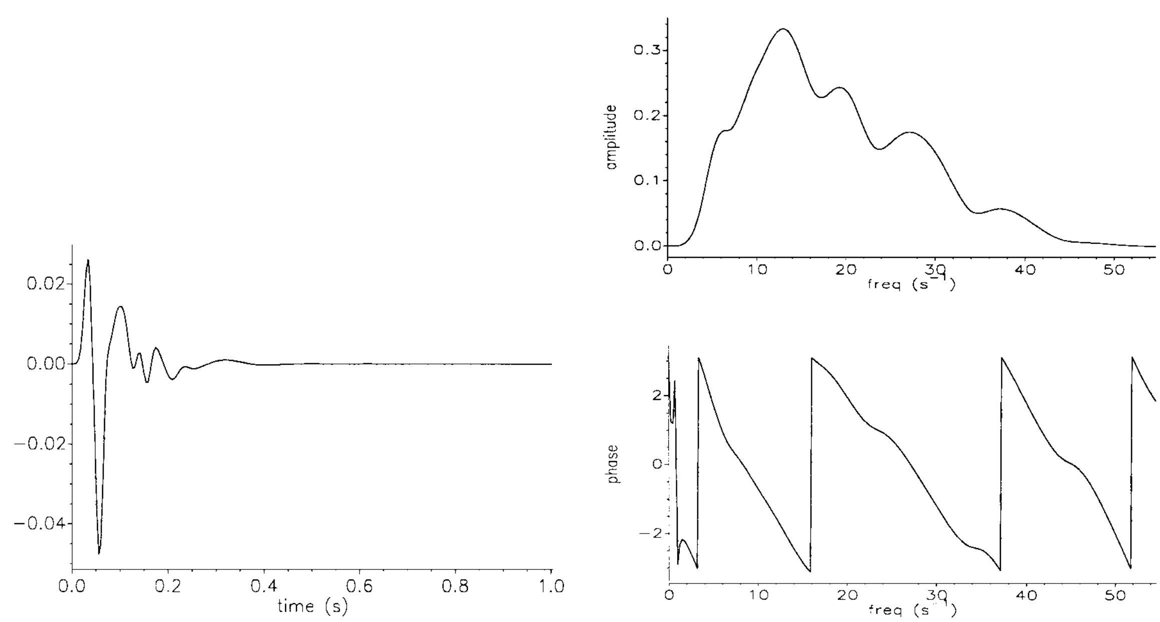

time domain representation *amplitude and phase spectrum*

FIG. 6. Air-gun–array wavelet that is used to bandlimit the seismic data of the subsurface model in Figure 5.

multiples with less moveout, compared to the first iteration result (Figure 12c). Apparently, because of a better initial estimate, the balance between different orders of predicted multiples is improved. The second iteration removes a small amount of additional multiple energy in the deeper part (e.g., at 3.1 s). This will be more evident on the stacked sections. To show the amount of multiple versus primary energy, Figure 13 illustrates the energy distribution, averaged over several shot gathers, before and after multiple elimination as a function of time. Clearly, the very large amount of multiple energy can be observed, especially in the deeper part of the section.

Figure 14 shows the stacked sections before multiple elimination, after the first iteration and after the second iteration. In addition, the difference sections between the iteration results and the input data are computed, showing the stack of the multiples. Note that the second iteration can be necessary for the deeper part of the section (e.g., note at 3.1 s more multiple energy is removed in the second iteration, as shown in Figure 14e).

Parabolic Radon output as initial primary estimate.—Next, we use the parabolic Radon output as an initial multiple-free estimate.

Figure 15b shows the output of Radon filtering (Figure 15a is just a repeat of the input data). Based on moveout, the Radon filtering procedure cannot separate primaries and multiples fully in the deeper part (>2.3 s). For comparison, Figure 15c shows the multiples removed with the Radon

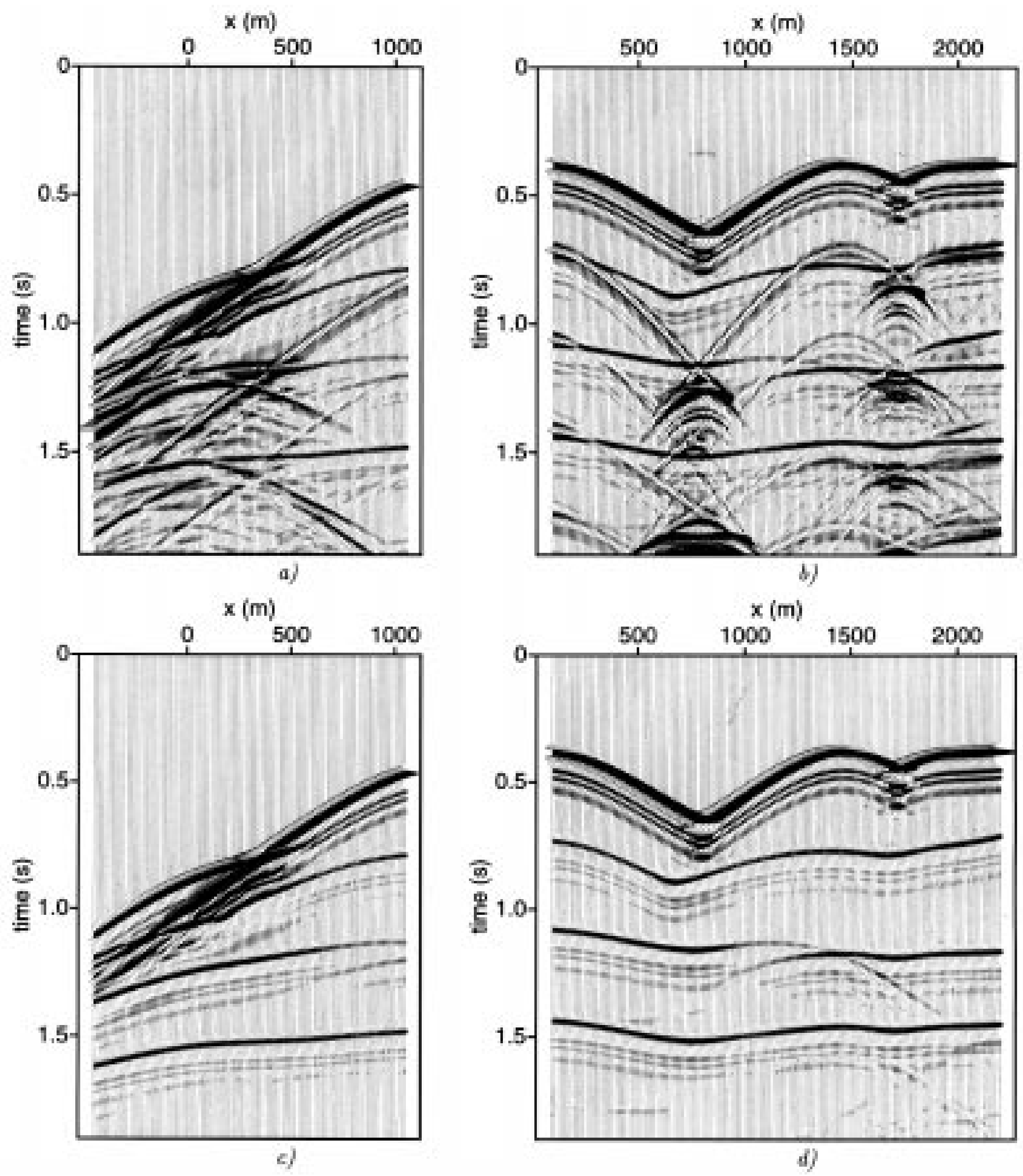

FIG. 7. Seismic data related to the model of Figure 5. (a) Shot record with the source at $x = 1050$ m, including multiples. (b) Zero-offset section, including multiples. (c) Shot record with the source at $x = 1050$ m without multiples. (d) Zero offset section without multiples.

method. Figure 15d displays the result of the first iteration using the Radon output as a multiple-free estimate and, again, we see that one iteration is already very good. Although the parabolic Radon result appears to be much "cleaner" than the surface-related multiple elimination, the Radon filtering procedure does not guarantee that the amplitude of the primary events are totally preserved. As already discussed, in the lower part, the Radon method is unable to remove the multiples that have similar moveouts as the primaries (e.g., at 3.1 s). Based on the subtracted multiple display (Figure 15e), the result is very similar to the two-iteration result using the input data as initial estimate (Figure 12e). Figure 16 shows the results for the stacked sections. As expected, in the deeper part the Radon result (Figure 16a) is not satisfactory; e.g., note that the focused multiple energy around CMP number 1030 could not be removed properly and the amount of removed multiples in the deeper part is small compared to the surface-related result. For the deeper part, application of the surface-related process is very important (e.g., the area around CMP 1200 below 2.5 s). After one iteration, based on the difference sections, the surface-related multiple result looks very similar (or even slightly better) to the previous two-iteration result (compare Figure 14e with Figure 16e for the data between 3.0 and 3.5 s).

The estimated global inverse source signatures have been displayed in Figure 17 for the situations with and without parabolic Radon filtering. It can be observed that independent of the initial estimate and iteration number, the phase spectrum is the same in all cases. However, the amplitude spectrum of

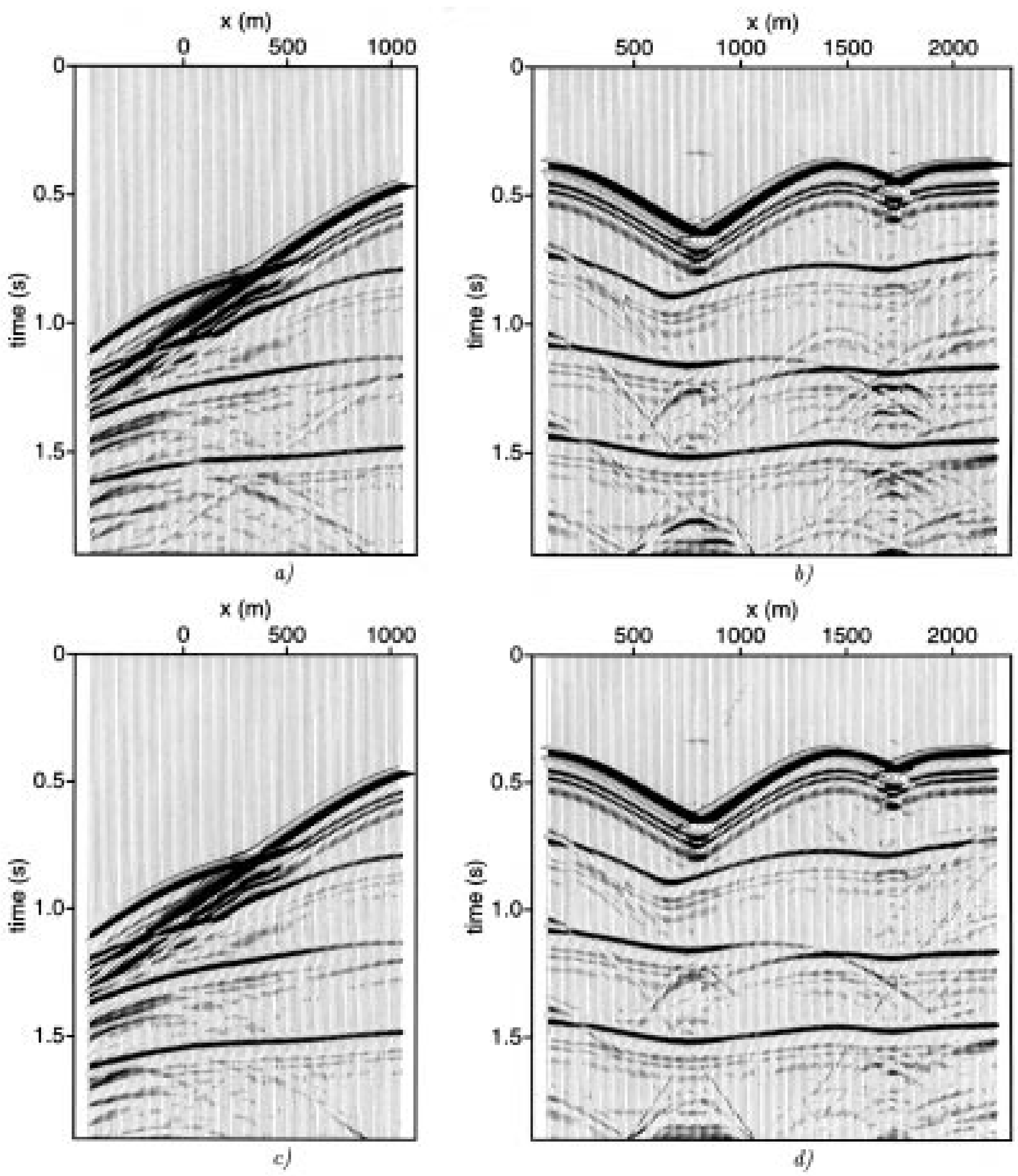

FIG. 8. Results of the multiple removal process, using the input data as initial estimate. Shot record (a) and zero offset section (b) after one iteration. Shot record (c) and zero offset section (d) after two iterations.

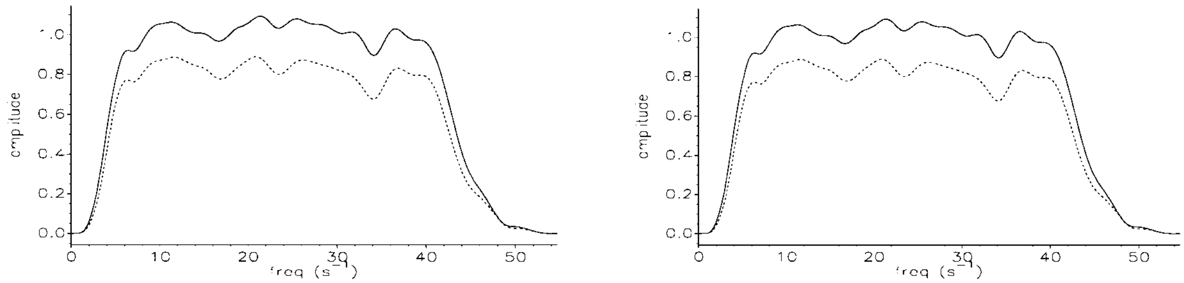

FIG. 9. Spectral properties of the deconvolution result (estimated inverse source signatures convolved with the original source wavelet) for iteration 1 (dashed line) and 2 (solid line).

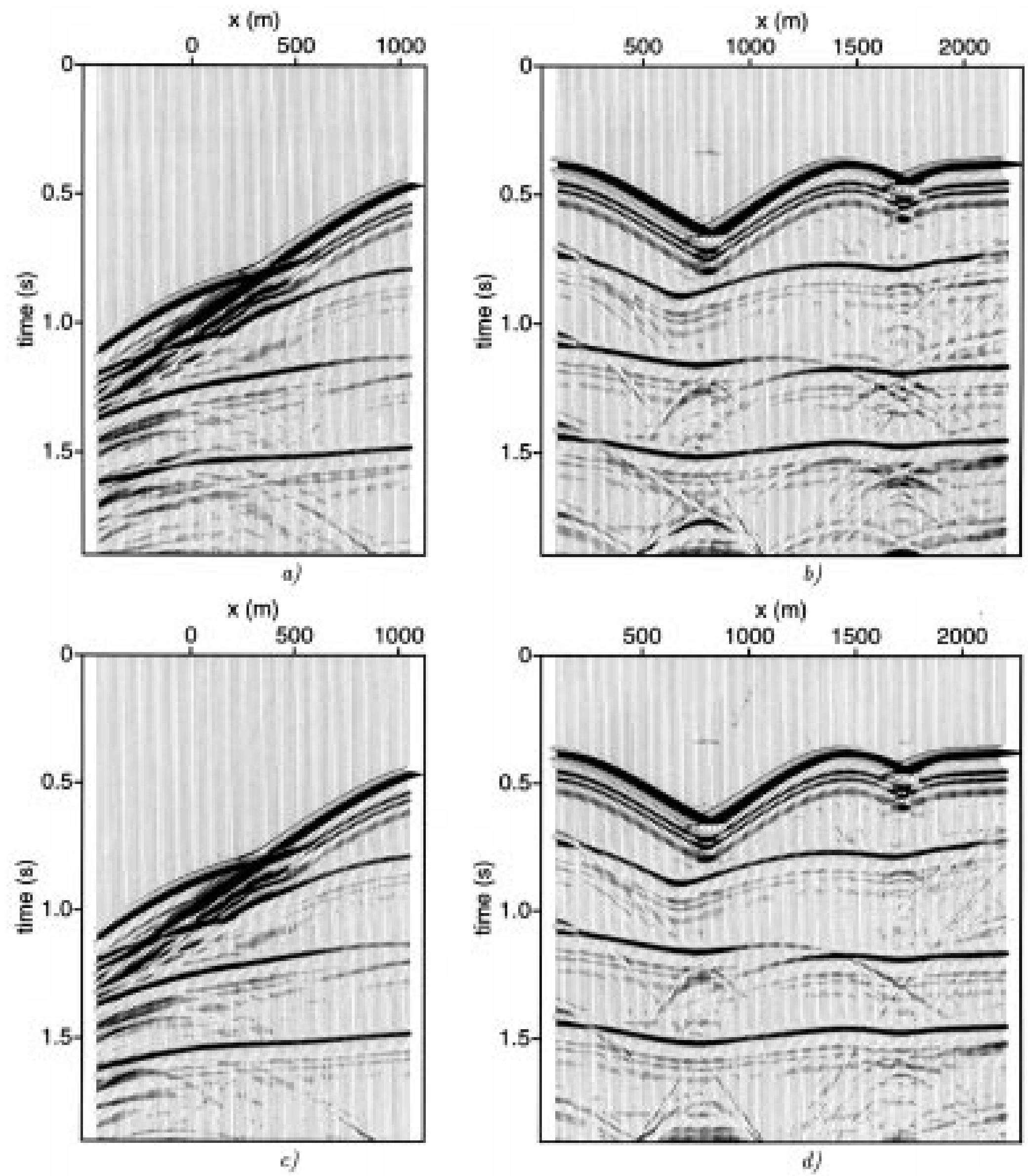

FIG. 10. Results of the multiple removal process, using the muted Radon data as initial estimate. First iteration result is shown in (a) and (b), and the second iteration result is shown in (c) and (d).

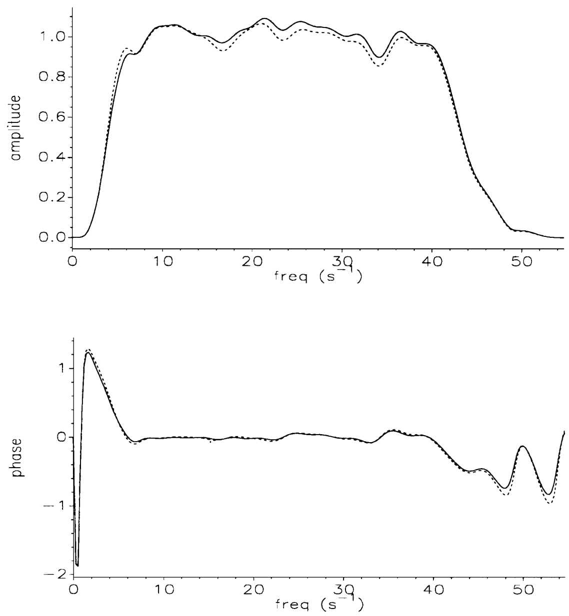

FIG. 11. Spectral properties of the deconvolution result (estimated inverse source signatures convolved with the original source wavelet) for iteration 1 (dashed line) and 2 (solid line) using the Radon filtered and muted input data as initial primary estimate.

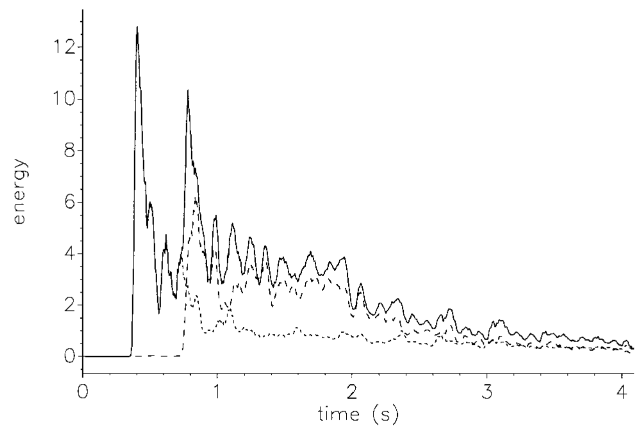

FIG. 13. Average prestack energy distribution as a function of time for the data with multiples (solid line), primaries only (dotted line), and multiples only (dashed line). Note that below 1 s the multiples contain more energy than the primaries.

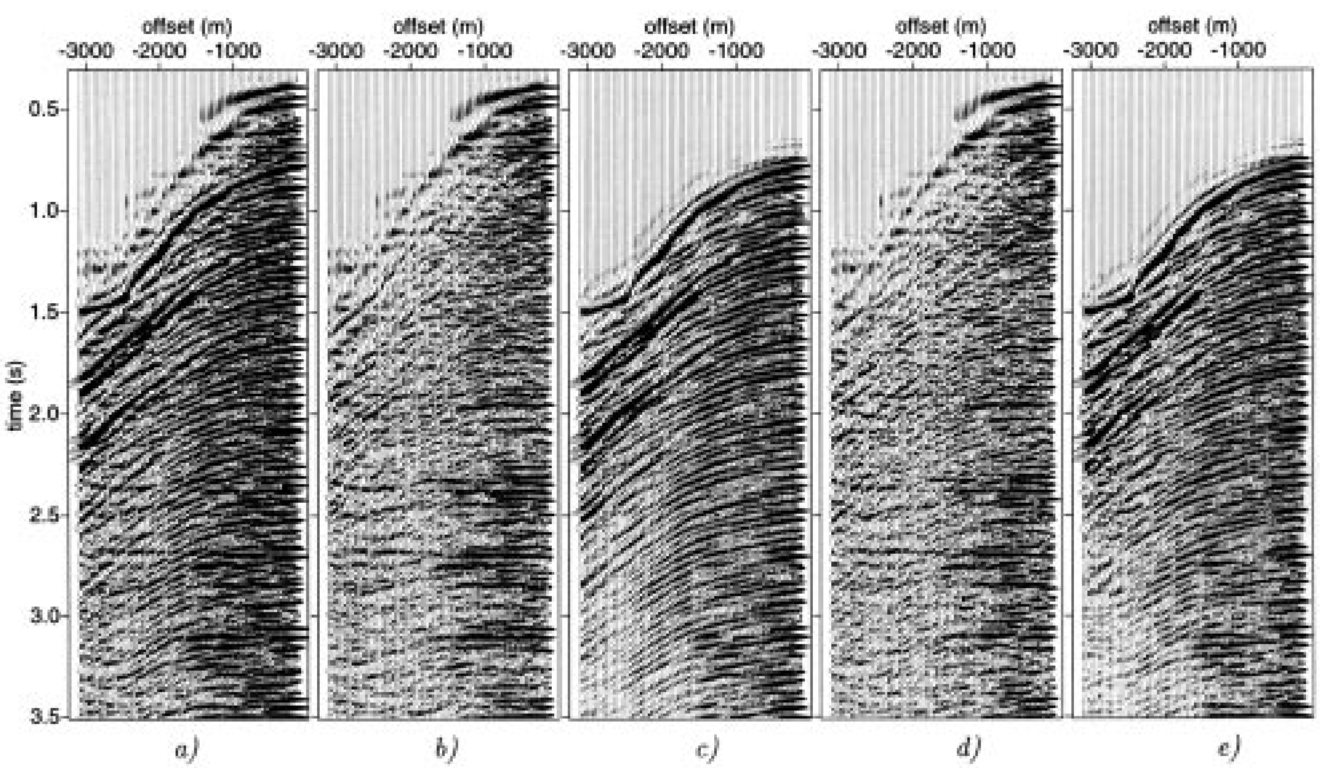

FIG. 12. Shot gather of a marine line. (a) Input. (b) Results of the first iteration of the multiple removal process, using the input data as initial estimate. (c) Difference of (a) and (b), i.e., the removed multiples. (d) Result after two iterations. (e) Multiples after two iterations. All gathers have been displayed after NMO correction and with the same amplitude.

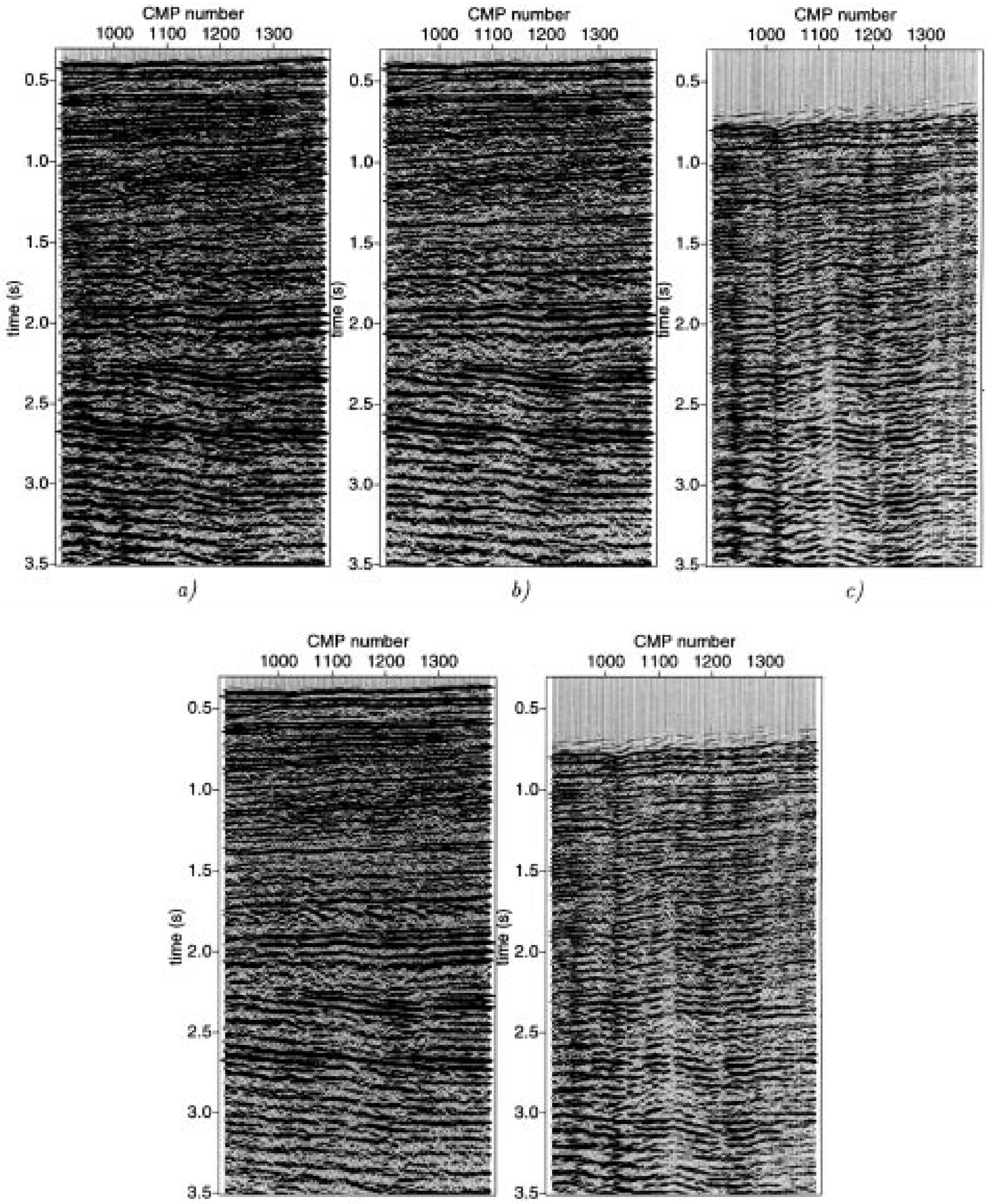

FIG. 14. (a) Stacked section of the marine data with multiples. (b) Stacked section after the first iteration result, using the input data as initial estimate. (c) Stack of multiples after one iterations, i.e., the difference between (a) and (b). (d) Stacked section of the second iteration result. (e) Multiples after two iterations, i.e., the difference between (a) and (d).

the inverse source signature is influenced by the initial estimate and the number of iterations (i.e., Figure 17a).

Middle East data set

As a last example, a data set from the Middle East area is considered, where the water depth is approximately 60 m. Here we will only consider the stacked results and use the input data as an initial multiple-free estimate. Figure 18a shows the stack of the data with multiples. A lot of ringing effects throughout the whole section can be observed. This area is known for having insufficient velocity discrimination for moveout-based multiple removal procedures. Therefore, surface-related multiple elimination seems to be a good candidate to solve the problem. Two iterations have been applied to this data, using the input data as multiple-free estimate. For the adaptive procedure, a two-stage adaptation is applied once again—first a global filter (21 points) and than 5-point filters within local time and offset windows (256 samples by 24 traces) for each shot record. Because of this adaptation procedure, the first iteration again shows good results, with additional improvements in the lower part when the second iteration is applied. This can be observed when comparing the difference sections, Figures 18d and 18e.

In both the field data examples, it is striking to see that the lateral behavior of the multiples on the stacked sections is much more fluctuating than the primary events. Small changes in reflector topography or reflectivity has an accumulating effect on the generated surface multiples (i.e., the ringing effect at CMP 1030 in Figure 14a and around CMP 2500 in Figure 18a).

CONCLUSIONS

1) The examples show that the iterative formulation of surface-related multiple removal, as described in part I of this paper, defines a fast-converging process. It is expected that in many situations one or two iterations are already sufficient.
2) The initial estimate has no effect on the end result (even a zero initial estimate can be used). It has an effect on the convergence rate only.
3) The simplest initial estimate of the multiple-free data equals the input data itself. Optionally, the (shallow) output of parabolic Radon filtering may be used to refine this initial estimate.
4) The surface-related multiple elimination process is very effective in the lower part of the section (say below 2 s), where the moveout properties of the primaries and multiples are generally very similar. In addition, the surface-related multiple-elimination process is very effective in situations with a complex multiple-generating system.
5) The surface-related multiple-elimination method is applied adaptively, yielding an estimate of the inverse source signature. Independent of the initial estimate and the number of iterations, the phase spectrum of the estimated inverse source signature is in all cases the same. This important property emphasizes the robustness of the method for getting accurate phase information on the source signature.

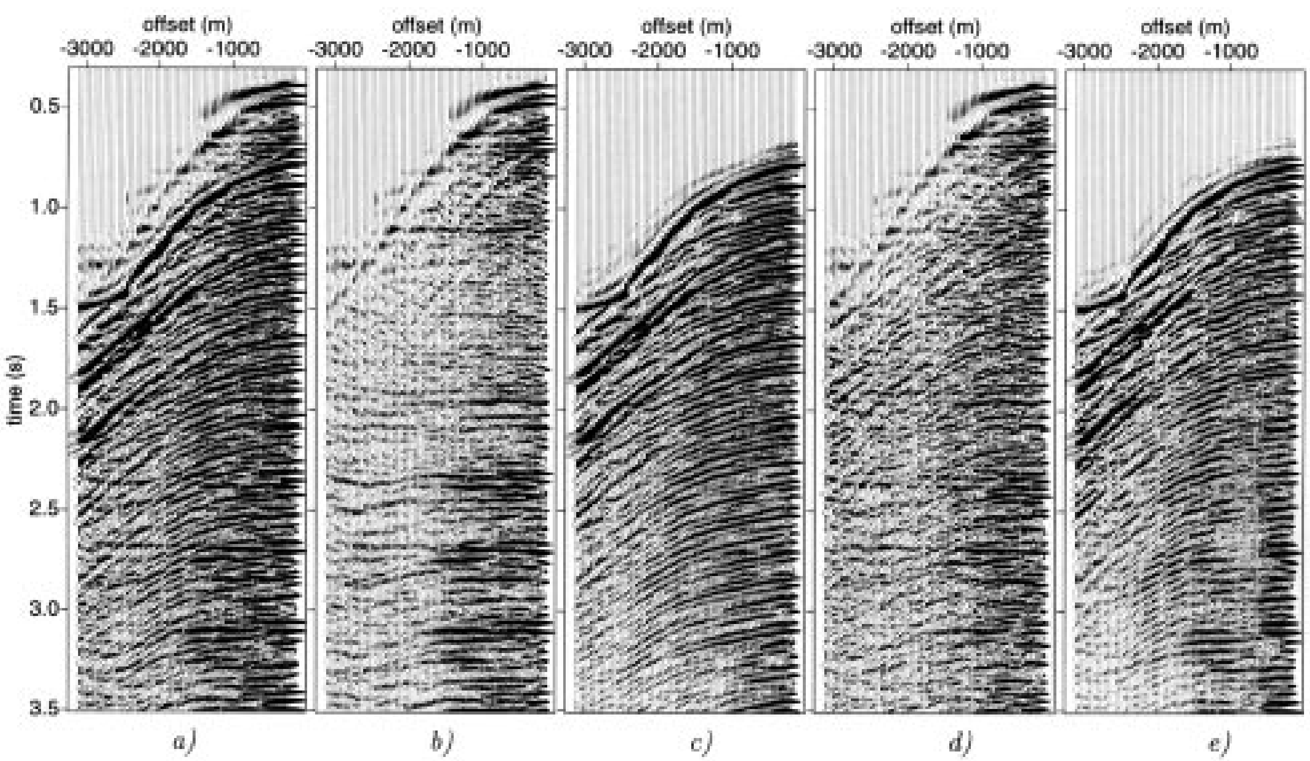

FIG. 15. Shot gather of a marine line. (a) Input. (b) Result of parabolic Radon multiple removal. (c) Difference of (a) and (b), i.e., the removed Radon multiples. (d) Results of the first iteration of the multiple removal process, using the Radon result as initial estimate. (e) Multiples after Radon multiple elimination and one iteration. All gathers have been displayed after NMO correction and with the same amplitude.

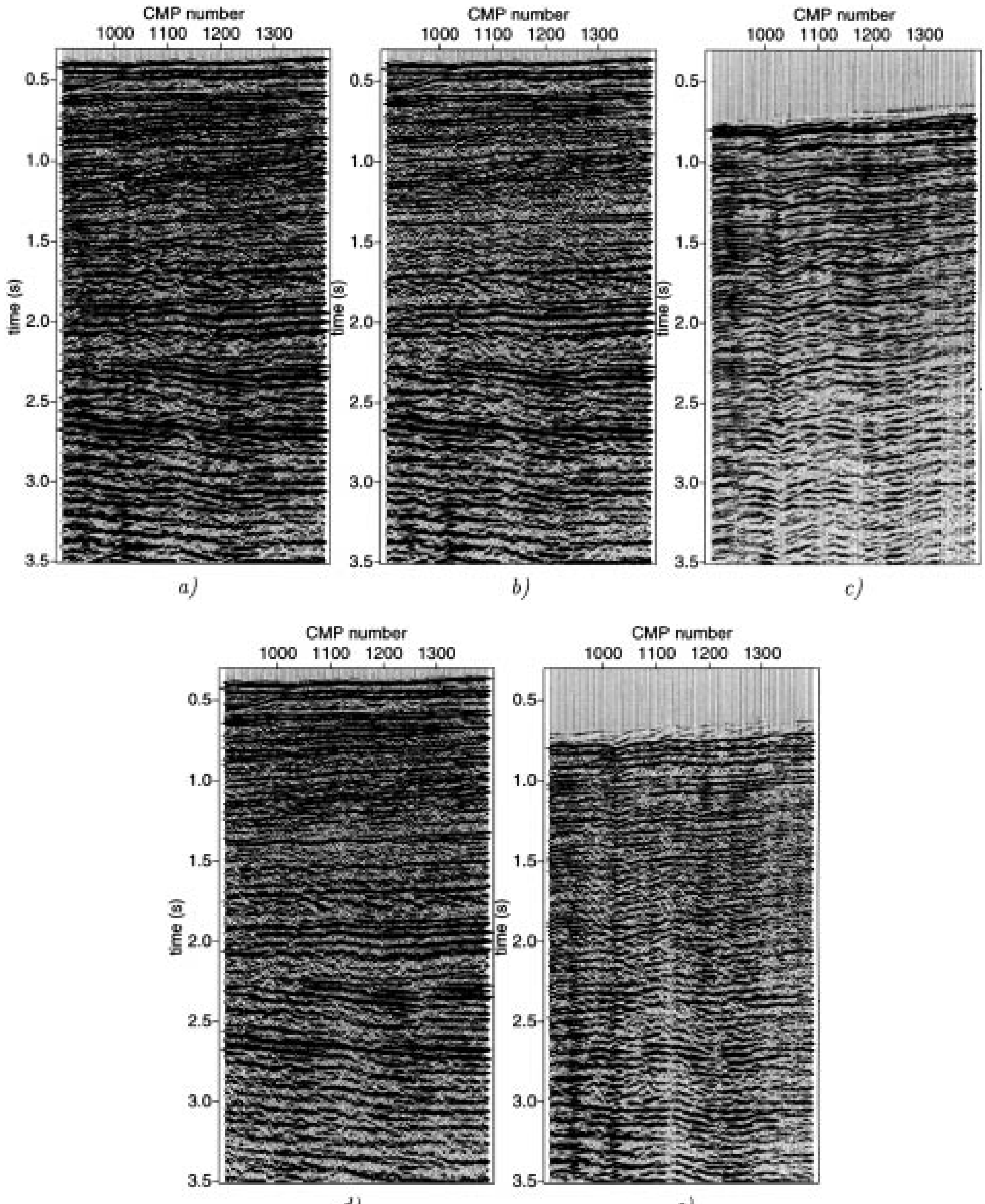

FIG. 16. (a) Stacked section of the marine data with multiples. (b) Stacked section of the marine data after parabolic Radon filtering. (c) Stack of the Radon removed multiples, i.e., the difference between (b) and (a). (d) Stacked section of the first iteration result, using the Radon output as initial an initial estimate. (e) Stack of multiples after one iteration using the Radon result as initial estimate, i.e., the difference between (d) and (a).

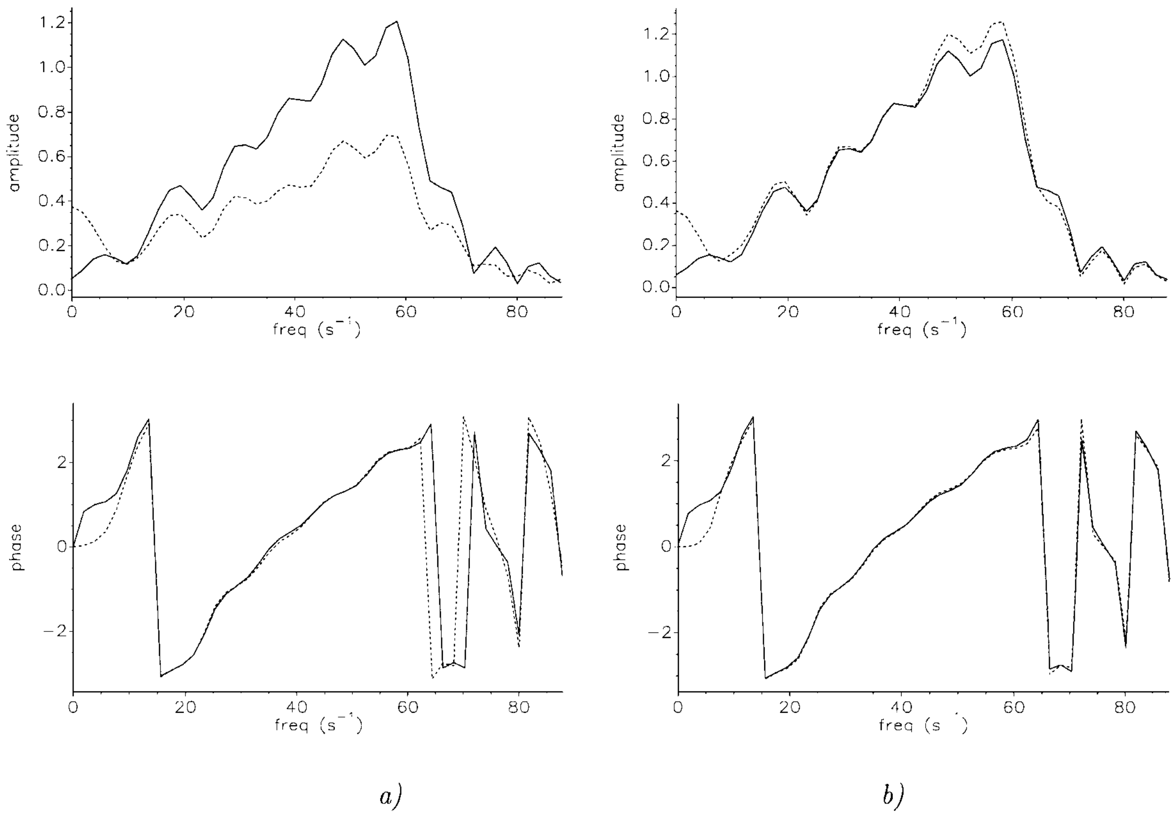

FIG. 17. Estimated inverse source signature after one (dashed line) and two (solid line) iterations. (a) Results using the input data as initial estimate. (b) Results using the parabolic Radon output as initial estimate.

FUTURE DEVELOPMENTS

For the future the following improvements can be considered:

1) Different subtraction techniques can be investigated. The Wiener-shaping filter is a choice that appears very powerful. However, other than the least-squares criterion can be thought of as a match for the predicted multiples to the data. Furthermore, this adaptation could be applied in different domains (e.g. $\tau - p$ domain).
2) The full subtraction procedure, taking shot and receiver variations into account [as defined by equation (6)], might be an interesting option for land data applications, or for marine situations where the assumption of stationary source and receiver characteristics is not valid and cannot be solved in another way.

FINAL REMARKS

From the field data example, it may be concluded that the parabolic Radon filtering does a very good job in the shallow part of the seismic data, where moveouts of primaries and multiples are generally well separated. This is the reason we used the (shallow) Radon output as an *operator* in the first iteration. However, optionally Radon filtering may also be used as a postprocessing step to further improve the final result at the shallow levels.

ACKNOWLEDGMENTS

The authors would like to thank the sponsors of the DELPHI consortium for their support, and Saga Petroleum A.S. for providing the field data from the North Sea. The research of Dr. Verschuur is financed by the Royal Netherlands Academy of Arts and Sciences.

REFERENCES

Anstey, N. A., and Newman, P., 1967, Part I: The sectional autocorrelogram and part II: The sectional retro-correlogram: Geophys. Prosp., **14**, 391–426.

Berkhout, A. J., 1982, Seismic migration, imaging of acoustic energy by wavefield extrapolation, A: Theoretical aspects: Elsevier.

Berkhout, A. J., and Verschuur, D. J., 1997, Estimation of multiple scattering by iterative inversion, Part I: Theoretical considerations Geophysics, **62**, 1586–1595.

Berryhill, J. R., and Kim, Y. C., 1986, Deep-water peg legs and multiples: Emulation and suppression: Geophysics, **51**, 2177–2184.

Fokkema, J. T., Baeten, G. J. M., and Vaage, S., 1990, Directional deconvolution in the f-x domain: 60th Ann. Internat. Mtg., Soc. Expl. Geophys., Expanded Abstracts, 1673–1676.

Hampson, D., 1986, Inverse velocity stacking for multiple elimination: J. Can. Soc. Expl. Geophys., **22**, No. 1, 44–55.

Kabir, M. M. N., and Verschuur, D. J., 1995, Restoration of missing offsets by parabolic radon transform: Geophys. Prosp., **43**, No. 3, 347–368.

Kennett, B. L. N., 1979, The suppression of surface multiples on seismic records: Geophys. Prosp., **27**, No. 3, 584–600.

Riley, D. C., and Claerbout, J. F., 1976, 2-d multiple reflections: Geophysics, **41**, No. 4, 592–620.

Robinson, E. A., and Treitel, S., 1980, Geophysical signal analysis: Prentice Hall, Inc.

Verschuur, D. J., Berkhout, A. J., and Wapenaar, C. P. A., 1992, Adaptive surface-related multiple elimination: Geophysics, **57**, No. 9, 1166–1177.

Wiggins, J. W., 1988, Attenuation of complex water-bottom multiples by wave-equation–based prediction and subtraction: Geophysics, **53**, 1527–1539.

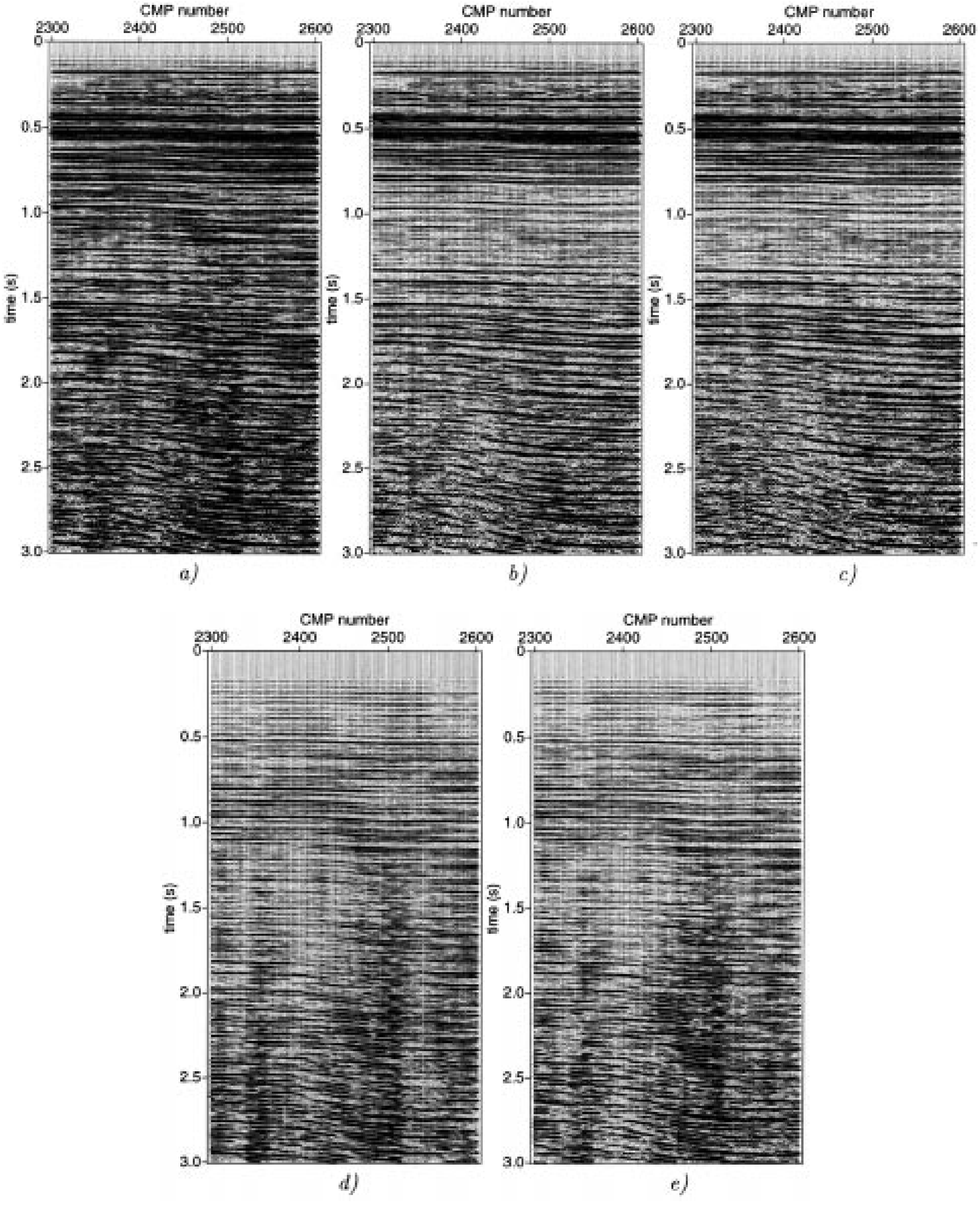

FIG. 18. Stacked sections from a marine line from the Middle East area. (a) Input data. (b) First iteration result, using the input data as multiple-free estimate. (c) Second iteration result. (d) Difference of (a) and (b), i.e., the removed multiples. (e) Removed multiples in the second iteration. All stacks have been displayed with the same amplitude scale.